Macromolecules

Article

pubs.acs.org/Macromolecules

From Spherical Micelles to Hexagonally Packed Cylinders: The Cure Cycle Determines Nanostructures Generated in Block Copolymer/Epoxy Blends

Hernán E. Romeo,*[,†] Ileana A. Zucchi,[†] Maite Rico,[‡] Cristina E. Hoppe,[†] and Roberto J. J. Williams*[,†]

[†]Institute of Materials Science and Technology (INTEMA), University of Mar del Plata and National Research Council (CONICET), J. B. Justo 4302, 7600 Mar del Plata, Argentina

[‡]Group of Polymers, Department of Physics, University of A Coruña, E.U.P Ferrol, Spain

ABSTRACT: Block copolymer (BCP)/epoxy blends have been intensively investigated during the past decade. Macrophase separation of the BCP in the cured thermoset is avoided by selecting one block that is initially immiscible or that phase separates early in the polymerization and another block that remains miscible up to high conversions. But the quality of the thermoset as a solvent of the miscible block varies along the cure cycle with both conversion and temperature. It shifts from a good solvent to a poor solvent, and eventually to a nonsolvent, by increasing conversion mainly due to the increase in the average molar mass before gelation and the cross-link density after gelation. It also changes with temperature due to the corresponding variation of the interaction parameter. Therefore, for a constant BCP concentration different nanostructures might be accessed and fixed by changing the cure cycle. This can be of interest to modulate final properties of the material (e.g., toughness, transparency, etc.). The selected system to prove this concept was a solution of 20 wt % PS-*b*-PMMA (M_n = 67 100, Φ_{PS} = 0.69) in a stoichiometric mixture of diglycidyl ether of bisphenol A (DGEBA) and 4,4′-methylenebis(2,6-diethylaniline) (MDEA). Generated nanostructures varied with the selected cure cycle from a dispersion of spherical micelles to a dual morphology consisting of domains of hexagonally packed cylinders and regions with a dispersion of spherical micelles. This produced changes in transparency and in dynamic-mechanical properties of the resulting nanocomposites.

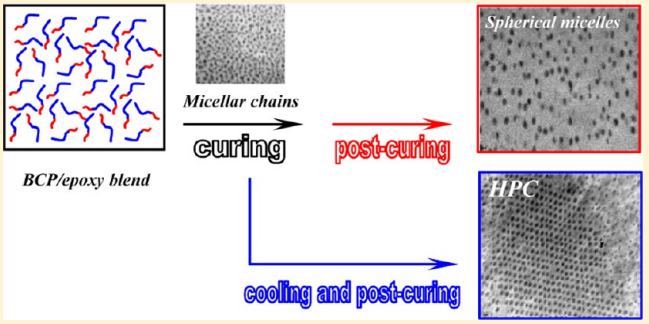

INTRODUCTION

The development of nanocomposite materials, in which the characteristic length scale of the filler is in the nanometer range, is currently one of the fastest growing areas of materials research.[1] In particular, polymer nanocomposites have expanded beyond their original scope (e.g., polymer-nanocrystal dispersions for refractive index tuning; clay-filled homopolymers for mechanical reinforcement) to include a wide range of new and outstanding applications.[2] These novel applications are a direct consequence of the exceptional control over size, shape, composition, and organization of the nanoscale domains arranged in the polymer matrix. However, the synthesis and characterization of these highly organized structures still remain challenging toward the development of next-generation materials and devices.[3,4]

Epoxy−amine systems are a class of important thermosetting polymers which have been widely employed as high-performance materials.[5] Over the past decades, considerable progress has been made on understanding the relationship between the morphologies and properties of multicomponent epoxy-based thermosetting blends.[6] Specifically, the morphological control of these thermosetting polymers at the nanometer level is long a pursuit in the studies of polymer science,[7] and it is consequently crucial to understand the mechanisms by which nanostructures can be accessed in these materials. In 1969, de Gennes proposed that nanostructured thermosets could be obtained via locking-in preformed ordered mesoscopic structures of the thermoset precursors via polymerization,[8] setting in this way the concept of "freezing" *in situ* preformed nanostructures by cross-linking. This concept was later taken by Bates et al., who proposed a novel strategy for creating nanostructures in thermosets using amphiphilic block copolymers (BCP).[9,10] BCP were self-assembled in reactive solvents generating different morphologies which were finally locked-in via cross-linking. This "self-assembly" (SA) approach, which has been widely accepted for the synthesis of nanostructured thermosets,[11−14] requires a block immiscible with the initial solvent and another block that is miscible up to high conversions. In some cases, a shift of the initial nanostructure in the phase diagram was observed at the end of the polymerization reaction.[9,10] Zheng and colleagues identified another mechanism known as reaction-induced microphase

Received: April 15, 2013
Revised: May 25, 2013

   dx.doi.org/10.1021/ma400778s | *Macromolecules* XXXX, XXX, XXX−XXX

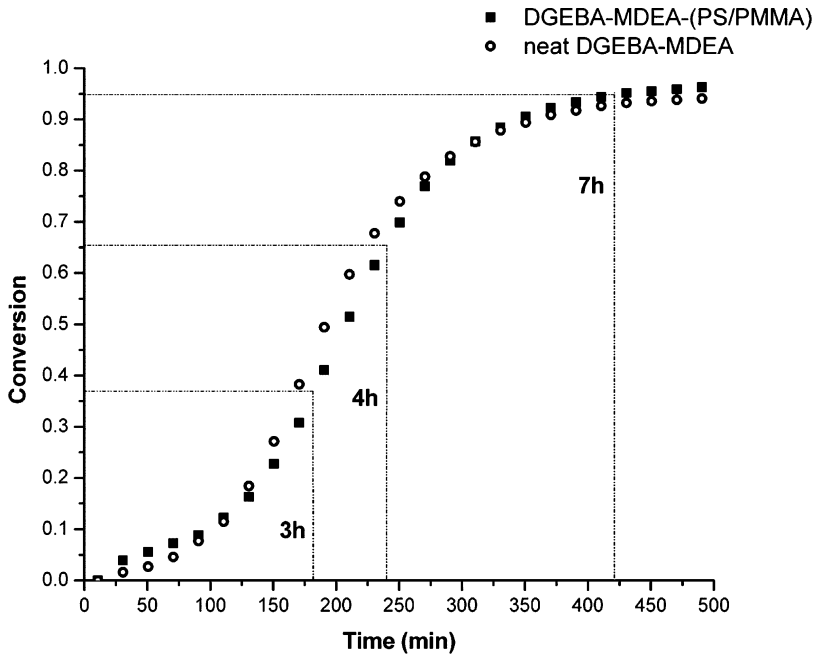

Figure 1. Conversion–time curves of the neat epoxy–amine formulation and the blend with 20 wt % PS-*b*-PMMA, cured at 135 °C.

separation (RIMPS), by which ordered copolymer morphologies can be accessed in epoxy-based systems.[15,16] In RIMPS both blocks are completely miscible with the initial reactive solvent, but one of them phase separates during polymerization while the other one remains miscible up to high conversions. Mechanistically, the formation of nanostructures via the SA approach is based on the equilibrium thermodynamics of the BCP/reactive solvent blend. On the contrary, the morphological control via RIMPS depends on the competitive kinetics between polymerization and microphase separation. This last aspect has been highlighted to be an asset over the SA process due to the tremendous versatility to modify the external parameters and consequently to modulate the resulting nanostructures.[16−20]

In this scenario there is one concept that has not been paid enough attention: the quality of the thermoset as a solvent of the miscible block changes with both conversion and temperature. It shifts from a good solvent to a poor solvent, and eventually to a nonsolvent, along polymerization due to the increase in the average molar mass before gelation (decrease in the entropic contribution to the free energy of mixing) and the increase in cross-link density after gelation.[21] These effects are much more significant than any change produced in the interaction parameter due to the modification of chemical structures.[21] But the quality of the solvent can be also modified by the selected cure cycle due to variations of the interaction parameter with temperature. Therefore, for a constant BCP concentration different nanostructures could be accessed in the course of polymerization, as shown in phase diagrams of solutions of BCP in selective solvents of different quality.[22−27] The possibility of trapping one of the evolving nanostructures generated during polymerization by control of the cure cycle can be of interest to modulate final properties of the material (e.g., toughness, transparency, etc.).

To the best of our knowledge, there is no previous study in the vast literature of BCP/epoxy blends showing that morphologies generated during polymerization of a specific blend can be significantly varied by selecting different cure cycles. The selected specific blend to prove this concept was a homogeneous solution containing 20 wt % PS-*b*-PMMA in a stoichiometric mixture of diglycidyl ether of bisphenol A (DGEBA) and 4,4′-methylenebis(2,6-diethylaniline) (MDEA). This formulation was chosen because it provided the versatility of RIMPS at a BCP concentration that could lead either to micellar dispersions or to ordered phases.

EXPERIMENTAL SECTION

Materials. The selected BCP was an asymmetric poly(styrene-*b*-methyl methacrylate) (PS-*b*-PMMA, Polymer Source, M_n = 67 100, Φ_{PS} = 0.69, PI = 1.07). The thermoset precursors were diglycidyl ether of bisphenol A (DGEBA, DER 332 Dow, with an epoxy equivalent of 348.6 g/mol) and 4,4′-methylenebis(2,6-diethylaniline) (MDEA, Aldrich). Tetrahydrofuran (THF) was employed to dissolve the BCP prior to the mixing with the epoxy resin. PMMA (Polymer Source, M_n = 21 500, PI = 1.4) and PS (Polymer Source, M_n = 45 000, PI = 1.05) homopolymers were also used to determine cloud-point times of homopolymer-modified systems in order to compare them with the one of the copolymer-modified blend.

PS-*b*-PMMA/Epoxy–Amine Blends. Proper amounts of PS-*b*-PMMA were first dissolved in THF to prepare materials containing 20 wt % BCP. In a typical synthesis, BCP (0.0723 g) was dissolved in THF (1 mL), and the solution was poured in a silicon mold containing DGEBA (0.2 g). Homogeneous blends were obtained after stirring at room temperature. The systems were then transferred to a hot plate (80 °C) to completely evaporate the solvent. Finally, a stoichiometric amount of MDEA (0.0891 g) was added while stirring until a homogeneous solution was obtained. Blends of homopolymers (PS or PMMA) in the thermoset precursors were prepared with a similar procedure.

The first step of the polymerization was performed at 135 °C, a temperature that was selected because it enabled to follow the development and evolution of nanostructures during a period of several hours up to the vitrification of the epoxy matrix. Samples reacted to different conversion levels at 135 °C were postcured by increasing temperature to 190 °C and keeping this value for 4 h, according to literature protocols.[28] Another set of samples, reacted to different conversion levels at 135 °C, was cooled to room temperature and then heated to 190 °C and postcured for 4 h.

dx.doi.org/10.1021/ma400778s | *Macromolecules* XXXX, XXX, XXX–XXX

Characterization Techniques. *Near-Infrared (NIR) Spectroscopy.* NIR spectroscopy was employed to determine conversion vs time curves at 135 °C for the neat epoxy−amine formulation and for the formulation containing the BCP. A Genesis II-Mattson device, equipped with a heated transmission cell (HT-32, Spectra Tech) with quartz windows (32 mm diameter, 0.5 lead spacer) and a programmable temperature controller (Omega, Spectra Tech, ΔT: ± 1 °C), was employed. The conversion of epoxy groups was followed by measuring the height of the absorption band at 4530 cm^{-1} with respect to the height of a reference band at 4620 cm^{-1}.[29]

Transmission Optical Microscopy (TOM). TOM was employed to determine cloud point times of modified epoxy−amine formulations during polymerization at 135 °C. A Leica DMLB microscope equipped with a hot stage (Linkam THMS 600) and a photodetector incorporated into the optical path of the microscope were used for this purpose. Samples were placed between two glasses using a 0.5 mm stainless-steel spacer.

Transmission Electron Microscopy (TEM). TEM images were recorded at room temperature using a JEOL 100CX device. Ultrathin sections (~60 nm thickness) were obtained employing an LKB ultramicrotome. In TEM images of the neat BCP, a morphology consisting of bright hexagonally packed PMMA cylinders in a dark PS matrix was observed without using any staining procedure. Therefore, in TEM images of the BCP/epoxy blend, PS was associated with the dark domains and PMMA/epoxy with the bright domains.

Small-Angle X-ray Scattering (SAXS). SAXS spectra were obtained *in situ* during the polymerization at 135 °C at the beamline SAXS 1 of the National Laboratory of Synchrotron Ligth (LNLS, Campinas, Brazil). The reacting mixture was placed in a cell sealed with Kallebrat film, and SAXS spectra were recorded every 15 min for a period of 7 h. Spectra were also recorded during the cooling to room temperature of the 7 h-reacted material. Apart from these dynamic experiments, the device was used to obtain SAXS spectra of blends previously cured using different thermal cycles. The scattering intensity (in arbitrary units) was recorded as a function of the scattering vector $q = (4\pi/\lambda) \sin \theta$, where λ is the radiation wavelength (1.55 Å) and 2θ the scattering angle.

Dynamic Mechanical Analysis (DMA). DMA 7 (PerkinElmer, Shelton, CT) of cured blends obtained with different thermal cycles was performed employing a tensile configuration. Specimens of 20 mm × 3 mm and 0.3 mm thickness were tested employing a heating rate of 10 °C/min.

RESULTS AND DISCUSSION

Conversion vs Time Curves at 135 °C. Figure 1 shows conversion vs time curves obtained at 135 °C for both the neat epoxy−amine formulation and the BCP-modified blend. The evolution of conversion was similar for both systems. Taking into account that the gel conversion for a stoichiometric DGEBA−aromatic diamine formulation is close to 0.60 (the ideal value is $x_{gel} = 0.577$; substitution effects increase this value to about 0.60),[30] three different cure times were selected (3, 4, and 7 h), corresponding to conversions respectively located before gelation ($x = 0.37$), after (but close to) gelation ($x = 0.65$), and close to vitrification ($x = 0.95$).

Miscibility of PS and PMMA Homopolymers during Polymerization. The miscibility of PS and PMMA homopolymers in the DGEBA−MDEA solvent was followed by transmission optical microscopy (TOM) during polymerization at 135 °C. For this purpose, homopolymers were selected with similar molar masses and used in equivalent concentrations (13.7 wt % PS and 6.3 wt % PMMA) as those present in the 20 wt % BCP blend.

For the PS−(DGEBA−MDEA) blend, a sharp decrease in transmittance was observed after 80 min reaction due to the phase separation of PS. The intensity of transmitted light increased slowly after this time as a result of the increase of the refractive index of the thermosetting polymer with conversion, matching the one of PS.[29,31−33]

In the case of blends containing the PMMA homopolymer, no variation in intensity was observed during the 7 h reaction at 135 °C. The cooling to room temperature of samples reacted to high conversions (postgel stage) did not show changes in transparency in the samples used in the TOM device. However, a barely discernible opalescence was observed in thick samples cooled to room temperature. This means that PMMA was close to the solubility limit in the 7 h-reacted blend. Cooling to room temperature led to a phase separation of PMMA due to its upper critical solution temperature (UCST) behavior in epoxy/amine reactive solvents.[31,34,35]

Evolution of Nanostructures Generated during Polymerization at 135 °C. *In situ* SAXS spectra recorded during polymerization at 135 °C are shown in Figure 2. The most

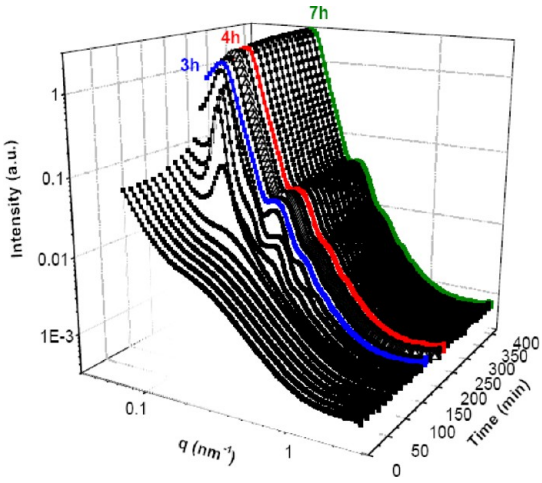

Figure 2. *In situ* SAXS spectra obtained during polymerization of the BCP/epoxy blend at 135 °C.

significant morphological changes were observed during the first 3 h. After this time, no significant changes in the spectra were observed except for a small increase in the intensity. The first significant change from the initial spectrum took place at 90 min when a small peak was generated that increased in intensity and shifted to lower q values with time. As phase separation of the PS homopolymer was detected at 80 min, the appearance of this peak in SAXS spectra was assigned to the generation of spherical micelles with PS cores and PMMA shells.

The following significant change in SAXS spectra was observed after about 2 h reaction. Figure 3 shows the SAXS spectrum recorded after 135 min reaction.

The presence of a high-intensity peak located at $q_0 = 0.1387$ nm^{-1} along with four low-intensity shoulders located at $q/q_0 = \sqrt{2}:\sqrt{3}:2:\sqrt{6}$ reveals the presence of a short-range cubic structure. The last shoulder is superimposed to the first maximum associated with the spherical form factor whose presence denotes the narrowing of the size distribution of the spherical micelles.[36] The spectrum might be assigned to a short-range body-centered cubic (bcc) arrangement of spherical micelles, in agreement with phase diagrams of BCP/epoxy−amine blends.[37]

As shown in Figure 4, the short-range order completely disappears after 3 h reaction. In the spectra obtained after 3 and 4 h, the pattern of the short-range cubic array was replaced by

dx.doi.org/10.1021/ma400778s | *Macromolecules* XXXX, XXX, XXX−XXX

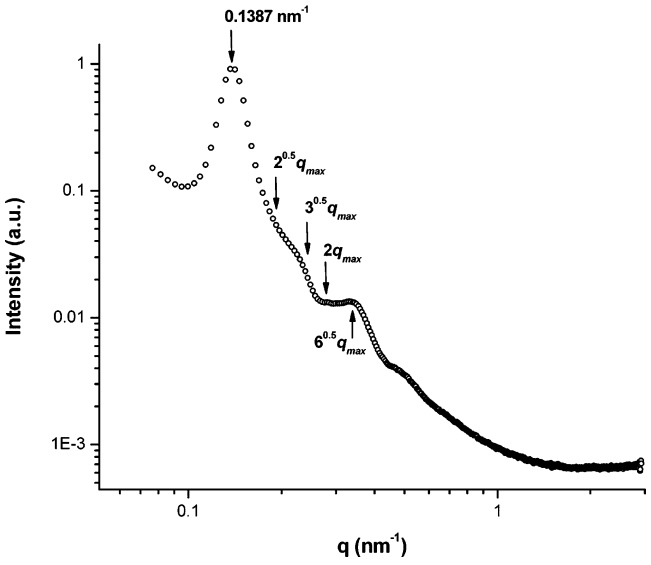

Figure 3. *In situ* SAXS spectra obtained after 135 min reaction of the BCP/epoxy blend at 135 °C.

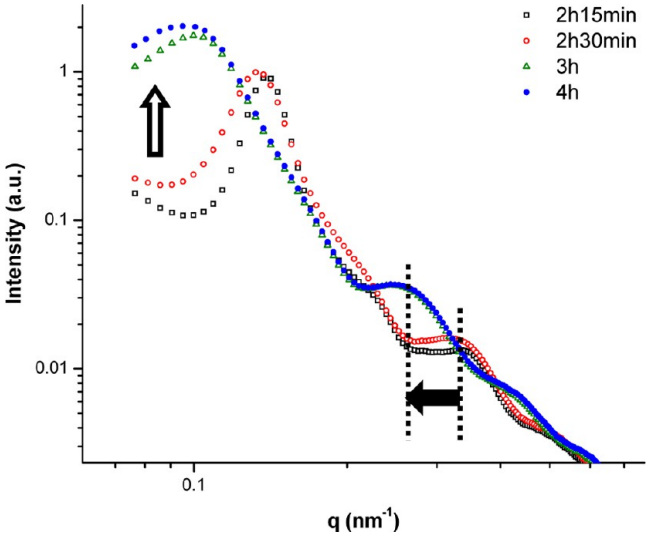

Figure 4. *In situ* SAXS spectra of BCP/epoxy blends obtained from 2 h 15 min to 4 h reaction.

the appearance of a broad and high-intensity peak at low q values (unfilled arrow) and the shift to lower q values of peaks initially present at higher q values (filled arrow). This represents a possible change of shape and increase in the size of the scattering objects (micelles) produced by decreasing the quality of the solvent with respect to the PMMA block.[38,39] A cooling stage from 135 °C to room temperature provided evidence of the shape of these micelles.

Evolution of Nanostructures Generated during Cooling to Room Temperature. BCP/epoxy blends were cured for 3, 4, and 7 h at 135 °C and were then cooled to room temperature in the silicon mold. The samples were transparent at 135 °C but became rapidly opaque during the cooling period. The transparent to opaque transition must be produced by the generation of BCP-rich domains of micrometer size that scattered visible light. These morphological changes should have their origin in the decrease of the miscibility of PMMA derived from its UCST behavior with epoxy/amine species. What was completely unexpected was to observe this transition in the sample cured for 7 h at 135 °C. This assay was repeated several times, and the experimental observation was always the same. The sample remained transparent at 135 °C but became opaque when the temperature reached about 110 °C in the cooling step. At this temperature the epoxy/amine matrix was already vitrified. Therefore, it must be accepted that the evolution of morphology was confined to the BCP-rich regions of the sample that still contained a fraction of residual monomers and oligomers that were partially deswollen during the cooling step. This generated significant changes in the organization of BCP domains which are described in what follows.

Figures 5 and 6 show TEM images of blends cured during different times at 135 °C and cooled in the silicon mold.

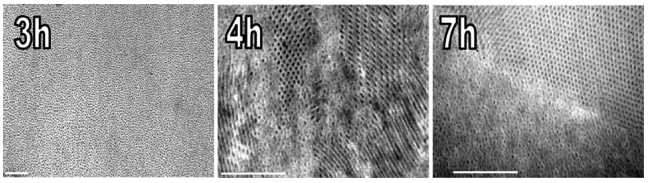

Figure 5. TEM images of PS-*b*-PMMA (20 wt %)/epoxy blends cured during different times in the silicon mold and cooled to room temperature. Bars = 1 μm.

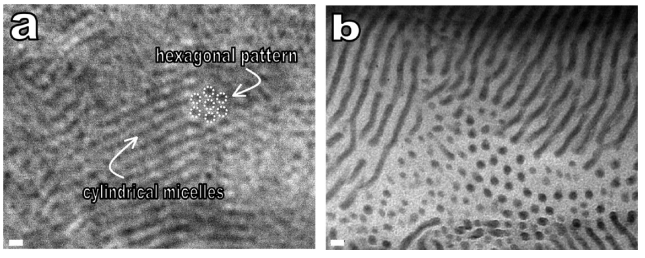

Figure 6. TEM images of PS-*b*-PMMA (20 wt %)/epoxy blends cured for 4 h at 135 °C and cooled to room temperature. Bars = 100 nm (images a and b correspond to two different regions at a similar magnification).

The 3 h cure led to a dense dispersion of chains of spherical micelles. A significant change of the nanostructure is observed in the blend cured for 4 h at 135 °C (a magnification of TEM images of this sample is shown in Figure 6). There are regions that kept the morphology of micellar chains shown in the 3 h-cured sample. But there are also microdomains where the BCP is present as long cylinders with a PS core and a PMMA shell that are self-assembled into an "inverted" hexagonally packed structure (inverted with respect to the one of the neat BCP). This results from the swelling of the PMMA block with the epoxy/amine solvent producing an inversion of the volume fraction of both phases. Inverted phases are characteristic of phase diagrams of BCP in selective solvents.[27] Cylindrical micelles generated by coalescence of micellar chains coexist with domains of hexagonally packed cylinders.

The following phase transitions—spherical micelles → bcc structure → chains of spherical micelles → cylindrical micelles → hexagonally packed cylinders—are the result of the decrease of the miscibility of the PMMA block in the epoxy/amine solvent, produced by the increase in conversion at 135 °C and the cooling step to room temperature. The intermediate generation of the bcc structure can explain the formation of the hexagonal phase as schematized in Figure 7. Micellar chains can

dx.doi.org/10.1021/ma400778s | *Macromolecules* XXXX, XXX, XXX−XXX

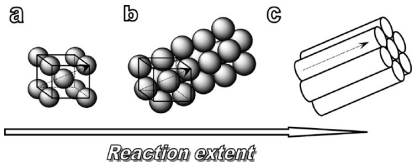

Figure 7. Schematic representation of the evolution of nanostructures during polymerization: (a) cubic array (bcc) of spherical micelles (the arrow shows the (111) direction), (b) micellar chains formed along the (111) direction of the bcc structure, and (c) hexagonally packed cylinders produced by the progressive transformation of micellar chains into cylinders.

be formed along the most compact (111) direction.[40] These micellar chains are progressively transformed into cylindrical micelles that are self-assembled into the hexagonal structure.

In the 7 h-cured sample a better degree of organization was achieved (Figure 5). Relatively large domains of hexagonally packed cylinders coexist with less organized regions exhibiting a dispersion of micellar chains.

Unfortunately, SAXS spectra of cooled samples did not show any evidence of the presence of the hexagonal phase, possibly due to its low volume fraction. Figure 8 shows SAXS spectra obtained *in situ* during the cooling to room temperature of the sample held for 7 h at 135 °C.

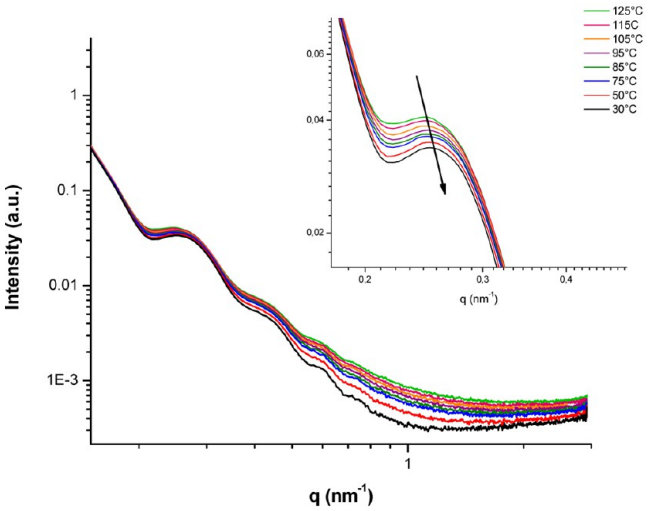

Figure 8. SAXS spectra recorded during the cooling to room temperature of a 7 h-reacted sample. The inset shows a magnification of the first maximum of the form factor.

The only significant change observed in the spectra was a shift of the maxima of peaks assigned to the form factor to higher q values. This indicates a decrease in the size of the scattering objects that can be associated with the sharper interface between PS and PMMA domains produced by the partial phase separation of PMMA from the epoxy/amine matrix. However, peaks corresponding to the hexagonal array are not present in the SAXS spectra possibly because they provide a weak contribution to the whole spectrum.

Nanostructures Present after the Post-Cure Stage at 190 °C. The effect of including or not a cooling step before the postcure step will be now analyzed. Figure 9 shows TEM images of the BCP/epoxy blend cured at 135 °C for 4 h, followed by a temperature increase to 190 °C and a 4 h postcure at this temperature.

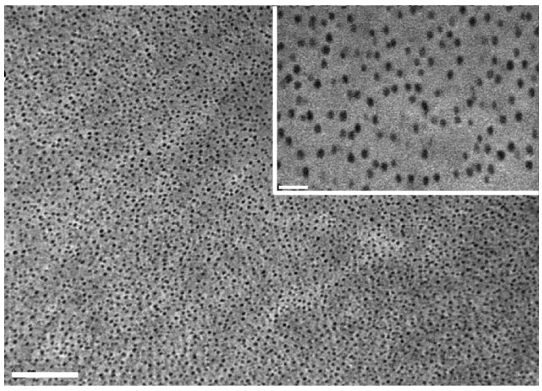

Figure 9. TEM images of PS-*b*-PMMA (20 wt %)/epoxy blend cured 4 h at 135 °C and postcured 4 h at 190 °C, without an intermediate cooling step. The inset depicts a magnification of the image. Bar = 1 μm (200 nm on the inset).

The cured blends were optically transparent and displayed a typical dispersion of spherical micelles with a PS core (black in the images) and a PMMA shell (undistinguished from the epoxy matrix). Chains of spherical micelles may be also distinguished in the TEM image. The average size of PS cores was $D \sim 40$ nm.

Figure 10 shows the SAXS spectrum of this blend. The q range was divided in two subranges: the one corresponding to

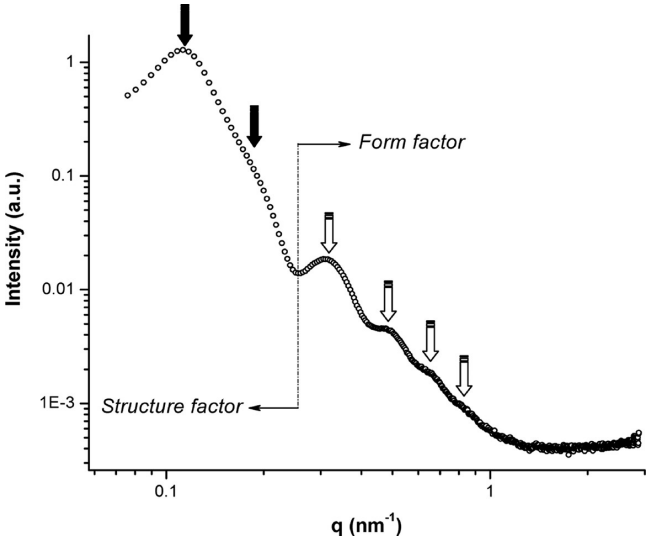

Figure 10. SAXS spectrum of PS-*b*-PMMA (20 wt %)/epoxy blend cured 4 h at 135 °C and postcured 4 h at 190 °C, without an intermediate cooling step.

the form factor contribution (from about 0.25 nm^{-1} to higher q values) and the one assigned to the structure factor (from about 0.25 nm^{-1} to lower q values). The form factor maxima (indicated with hollowed arrows) were correlated with a diluted system of spherical scattering domains with hard radius (R), where maxima are located at qR = 5.76, 9.10, 12.3, etc.[36,41] Using the value of the first maximum located at q = 0.31 nm^{-1} gives D = 37 nm, in close agreement with the average size obtained by TEM.

In the range of low q values, a broad scattering peak (q = 0.11 nm^{-1}) with a shoulder (identified with filled arrows) is present. This is assigned to a short-range ordering of the dispersion of

dx.doi.org/10.1021/ma400778s | *Macromolecules* XXXX, XXX, XXX−XXX

spherical micelles. The location of the maximum corresponds to a nearest-neighbor distance close to 57 nm.

We will now analyze the influence of a cooling step to room temperature previous to the postcure at 190 °C. Figure 11

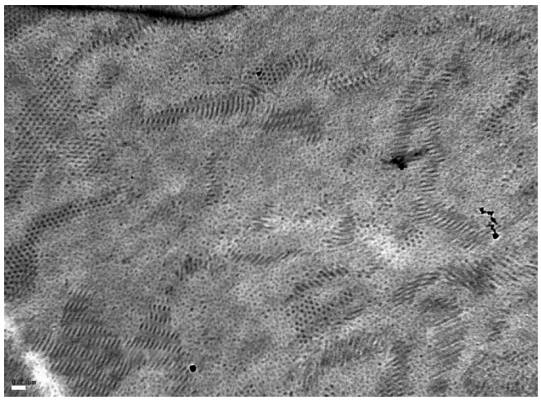

Figure 11. TEM image of a blend cured 4 h at 135 °C, cooled to room temperature, and postcured 4 h at 190 °C. Bar: 200 nm.

shows a TEM image of a blend cured 4 h at 135 °C, cooled to room temperature, and postcured 4 h at 190 °C. Microdomains of the hexagonal phase survived the temperature increase to 190 °C and were kinetically trapped in the final nanocomposite. This was also revealed by the fact that the sample remained opaque after the postcure steps. On the basis of these results, we can speculate that the hexagonal phase was generated during the cooling stage to room temperature by the local organization of pre-existing micellar chains and short cylindrical micelles present in the sample cured 4 h at 135 °C.

Figure 12 shows the morphologies obtained after the 4 h postcure at 190 °C of a blend previously reacted for 7 h at 135

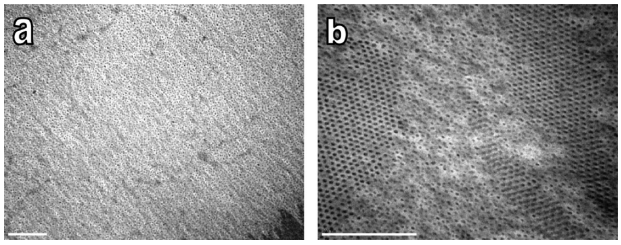

Figure 12. TEM images of a BCP/epoxy blend reacted for 7 h at 135 °C and 4 h at 190 °C: (a) without the intermediate cooling to room temperature; (b) with intermediate cooling to room temperature. Bars: 1 μm.

°C, with and without an intermediate cooling step to room temperature.

A similar situation to the one of the sample reacted for 4 h at 135 °C is observed. The absence of a cooling step led to a dispersion of spherical micelles and micellar chains. The introduction of a cooling step in the cure cycle led to a dual-phase morphology consisting of microdomains of the hexagonal phase and regions exhibiting a dispersion of spherical micelles and micellar chains. The sample that was not previously cooled was transparent while the other one was opaque.

Thermal-Mechanical Properties of Nanocomposites with Different Nanostructures. The introduction of a cooling step in the cure cycle did not only affect the resulting nanostructures but also produced a significant change of thermal-mechanical properties.

Figure 13 shows the loss peak as a function of temperature for the neat epoxy matrix cured for 7 h at 135 °C and cooled to

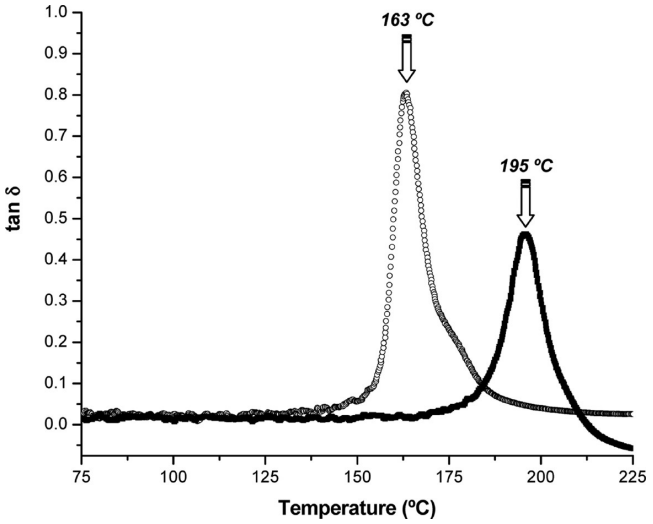

Figure 13. Tan δ as a function of temperature for the neat epoxy matrix cured for 7 h at 135 °C and cooled to room temperature (hollowed circles) and the sample cured for 7 h at 135 °C and postcured for 4 h at 190 °C (filled squares).

room temperature, and the neat epoxy cured for 7 h at 135 °C and postcured for 4 h at 190 °C (the intermediate cooling to room temperature did not produce any significant change in the resulting spectra).

The peak at about 163 °C corresponds to the relaxation of the epoxy matrix reacted to a conversion of 0.95 at 135 °C. The postcure for 4 h at 190 °C led to a fully converted (according to FTIR determinations) and homogeneous matrix with a structure characterized by a relaxation at about 195 °C. A small increase in conversion toward the end of polymerization produced a large increase of the glass transition temperature as is typical for epoxy−aromatic amine networks.

Figure 14 shows the loss peak as a function of temperature for BCP/epoxy blends polymerized for 7 h at 135 °C and subjected to different thermal treatments.

The sample cured for 7 h at 135 °C and cooled to room temperature displayed two distinct relaxations. The peak at 165 °C is assigned to the relaxation of the epoxy matrix that vitrified in the course of polymerization. The maximum of this peak was higher by 2 °C than the one of the neat epoxy cured under the same conditions (Figure 13). There are two factors that could have shifted this peak with respect to the one of the neat epoxy. The partial plasticization of the epoxy with PMMA would have shifted the relaxation to lower temperatures. But, at the same time, it would have delayed vitrification at 135 °C, enabling to attain a higher conversion than that of the neat epoxy (a small increase in conversion above 0.95 has a large effect on the shift of the relaxation peak, as shown in Figure 13). Both effects are almost counterbalanced, leading to similar locations of the high-temperature relaxation peak in the neat epoxy and in the BCP/epoxy blend. The broad low-temperature relaxation centered at about 130 °C is assigned to the overlapped relaxations of both PS and PMMA segregated domains. The partial microphase separation of the syndiotactic PMMA block was previously reported for other BCP/epoxy blends.[18]

dx.doi.org/10.1021/ma400778s | *Macromolecules* XXXX, XXX, XXX−XXX

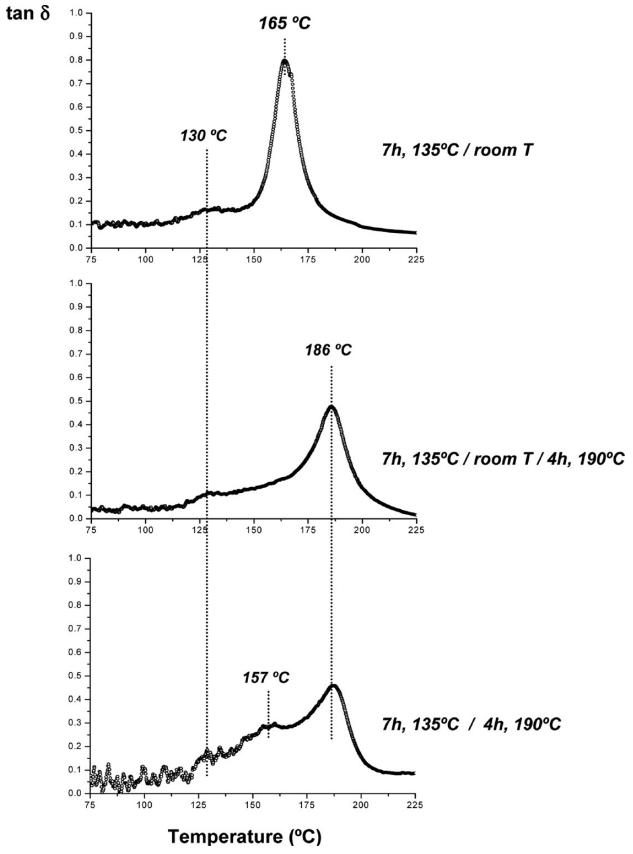

Figure 14. Tan δ as a function of temperature for BCP/epoxy blends subjected to different thermal treatments.

The postcure step produced different thermal-mechanical properties, depending on the presence or absence of a previous cooling step to room temperature. In both cases the relaxation of the epoxy matrix increased to 186 °C, a value that is 9 °C lower than the one of the neat epoxy cured with the same thermal cycle (Figure 13). This could be ascribed to the plasticization effect of a residual amount of PMMA blocks still dissolved in the epoxy matrix. Large temperature variations produced by the plasticization of an epoxy with PMMA have been previously reported.[42] The most significant change in the dynamic-mechanical spectra is the presence of a broad and continuous relaxation covering the temperature range located between the relaxations of the BCP and the plasticized epoxy matrix, observed for the blend postcured at 190 °C without the intermediate cooling step. This relaxation is assigned to a broad interface of PMMA/epoxy, with no epoxy at the interface with PS and a maximum epoxy fraction at the extreme of the PMMA blocks (a scheme that is plausible for a very dense micellar concentration). The introduction of a cooling step produced a larger deswelling of PMMA blocks, generating a sharper interface.

Figure 15 shows the storage modulus vs temperature for the neat epoxy and BCP/epoxy blends, cured for 7 h at 135 °C and 4 h at 190 °C, with and without an intermediate cooling to room temperature (for the neat epoxy, the intermediate cooling step did not produce any significant change).

As already discussed in relation to Figure 14, devitrification of BCP/epoxy blends was observed at lower temperatures, a fact assigned to the partial plasticization of the epoxy with PMMA. A significant increase of the glassy modulus is observed

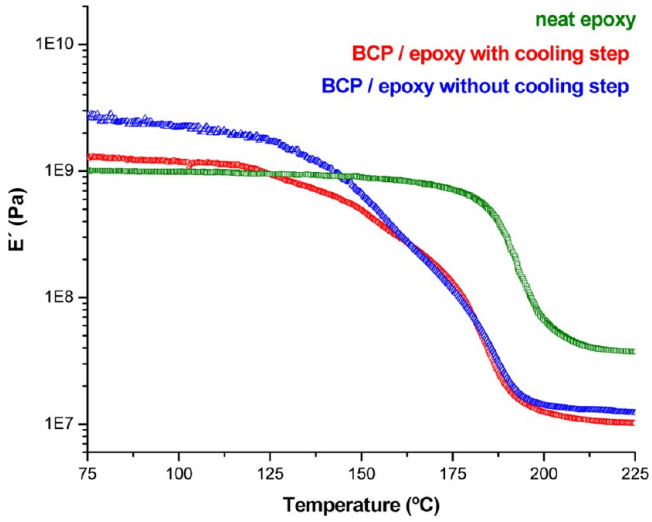

Figure 15. Storage modulus as a function of temperature for postcured samples. Green curve: neat epoxy matrix cured 7 h at 135 °C and postcured 4 h at 190 °C; Red curve: BCP/epoxy blend cured 7 h at 135 °C, cooled to room temperature and postcured 4 h at 190 °C. Blue curve: BCP/epoxy blend cured 7 h at 135 °C and postcured 4 h at 190 °C.

for the blend postcured without an intermediate cooling step. This can be related to the increase in cohesion produced by the broad interface of variable composition, extending from the PS−PMMA interface to the bulk matrix. In the rubbery region, devitrification of both blocks of the BCP produced a significant decrease of the rubbery modulus as previously reported for thermoplastic-modified epoxies.[42]

CONCLUSIONS

It was shown that a specific BCP/epoxy blend consisting of 20 wt % PS-*b*-PMMA dissolved in a stoichiometric mixture of diglycidyl ether of bisphenol A (DGEBA) and 4,4′-methylenebis(2,6-diethylaniline) (MDEA) produced the following sequence of nanostructures during polymerization at 135 °C: spherical micelles → bcc structure → chains of spherical micelles → cylindrical micelles. When these partially reacted materials were postcured at 190 °C without an intermediate cooling step, transparent blends exhibiting a dense dispersion of spherical micelles were obtained. Therefore, typical cure cycles defined by a partial advance in conversion at 135 °C followed by a postcure step at 190 °C led to similar final morphologies, erasing the previous evolution of nanostructures. This was the result of the increase of the miscibility of the PMMA block produced by the temperature increase, a fact that stabilized the dispersion of spherical micelles. Introducing an intermediate cooling step in the cure cycle enabled to continue the evolution of nanostructures in the following sequence: chains of spherical micelles → cylindrical micelles → hexagonally packed cylinders. This was explained by the decrease of the miscibility of the PMMA block produced during the cooling step. Opaque materials were generated which retained the ordered phase even after the postcure step at 190 °C. Besides, the introduction of the intermediate cooling step produced significant changes in the dynamic-mechanical spectra of the postcured blends. The cooling step favored the deswelling of PMMA and generated a sharper interface between the BCP and the bulk epoxy. In the absence of an intermediate cooling, a broad and continuous interphase was

dx.doi.org/10.1021/ma400778s | *Macromolecules* XXXX, XXX, XXX−XXX

generated between the PS core and the bulk epoxy. This produced a significant increase of the glassy modulus with respect to the one of the blend subjected to a cooling step.

In conclusion, it was proved that it is possible to generate different nanostructures in a specific BCP/epoxy blend simply by varying the cure cycle. This concept can be extended to any type of BCP/thermosetting polymer blends. Work is in progress in this direction.

AUTHOR INFORMATION

Corresponding Author

*E-mail: hromeo@fi.mdp.edu.ar (H.E.R.); williams@fi.mdp.edu.ar (R.J.J.W.).

Notes

The authors declare no competing financial interest.

ACKNOWLEDGMENTS

The financial support of the following institutions is gratefully acknowledged: National Research Council (CONICET, Argentina), National Agency for the Promotion of Science and Technology (ANPCyT, Argentina), and University of Mar del Plata. The grant SAXS1-13459 from the Brazilian Synchrotron Light Laboratory (LNLS, Campinas-SP, Brazil) is gratefully acknowledged. Maite Rico acknowledges a grant from Santander Bank for a postdoctoral stage at INTEMA.

REFERENCES

(1) Bockstaller, M. R.; Mickiewicz, R. A.; Thomas, E. L. *Adv. Mater.* **2005**, *17*, 1331.
(2) Ji, S.; Liu, C. C.; Liao, W.; Fenske, A. L.; Craig, G. S. W.; Nealey, P. F. *Macromolecules* **2011**, *44*, 4291.
(3) Daga, V. K.; Watkins, J. J. *Macromolecules* **2010**, *43*, 9990.
(4) Lin, Y.; Daga, V. K.; Anderson, E. R.; Gido, S. P.; Watkins, J. J. *J. Am. Chem. Soc.* **2011**, *133*, 6513.
(5) Zheng, S. In *Epoxy Polymers, New Materials and Innovations*; Pascault, J. P., Williams, R. J. J., Eds.; Wiley-VCH: Weinheim, 2010; p 81.
(6) Pascault, J. P.; Williams, R. J. J. In *Polymer Blends*; Paul, D. R., Bucknall, C. B., Eds.; John Wiley & Sons, Inc.: New York, 2000; p 379.
(7) Guo, Q. In *Polymer Blends and Alloys*; Shonaik, G. O., Simon, G., Eds.; Marcel Dekker: New York, 1999; p 155.
(8) de Gennes, P. G. *Phys. Lett.* **1969**, *28A*, 725.
(9) Hillmyer, M. A.; Lipic, P. M.; Hajduk, D. A.; Almdal, K.; Bates, F. S. *J. Am. Chem. Soc.* **1997**, *119*, 2749.
(10) Lipic, P. M.; Bates, F. S.; Hillmyer, M. A. *J. Am. Chem. Soc.* **1998**, *120*, 8963.
(11) Guo, Q.; Thomann, R.; Gronski, W. *Macromolecules* **2002**, *35*, 3133.
(12) Guo, Q.; Thomann, R.; Gronski, W. *Macromolecules* **2003**, *36*, 3635.
(13) Rebizant, V.; Venet, A. S.; Tournillhac, F.; Girard-Reydet, E.; Navarro, C.; Pascault, J. P.; Leibler, L. *Macromolecules* **2004**, *37*, 8017.
(14) Wu, J.; Thio, Y. S.; Bates, F. S. *J. Polym. Sci., Part B: Polym. Phys.* **2005**, *43*, 1950.
(15) Meng, F.; Zheng, S.; Zhang, W.; Li, H.; Liang, Q. *Macromolecules* **2006**, *39*, 711.
(16) Meng, F.; Zheng, S.; Li, H.; Liang, Q.; Liu, T. *Macromolecules* **2006**, *39*, 5072.
(17) Yu, R.; Zheng, S. *Macromolecules* **2011**, *44*, 8546.
(18) Ritzenthaler, S.; Court, F.; Girard-Reydet, E.; Leibler, L.; Pascault, J. P. *Macromolecules* **2003**, *36*, 118.
(19) Fan, W.; Zheng, S. *Polymer* **2008**, *49*, 3157.
(20) Fan, W.; Wang, L.; Zheng, S. *Macromolecules* **2009**, *41*, 327.
(21) Williams, R. J. J.; Rozenberg, B. A.; Pascault, J. P. *Adv. Polym. Sci.* **1997**, *128*, 95.
(22) Shibayama, M.; Hashimoto, T.; Kawai, H. *Macromolecules* **1983**, *16*, 16.
(23) Hashimoto, T.; Shibayama, M.; Kawai, H.; Watanabe, H.; Kotaka, T. *Macromolecules* **1983**, *16*, 361.
(24) Hanley, K. J.; Lodge, T. P. *J. Polym. Sci., Part B: Polym. Phys.* **1998**, *36*, 3101.
(25) Hanley, K. J.; Lodge, T. P.; Huang, C. I. *Macromolecules* **2000**, *33*, 5918.
(26) Lodge, T. P.; Pudil, B.; Hanley, K. J. *Macromolecules* **2002**, *35*, 4707.
(27) Suo, T.; Yan, D.; Yang, S.; Shi, A.-C. *Macromolecules* **2009**, *42*, 6791.
(28) Zucchi, I. A.; Galante, M. J.; Williams, R. J. J.; Franchini, E.; Galy, J.; Gerard, J.-F. *Macromolecules* **2007**, *40*, 1274.
(29) Zucchi, I. A.; Galante, M. J.; Williams, R. J. J. *Polymer* **2005**, *46*, 2603.
(30) Pascault, J. P.; Sautereau, H.; Verdu, J.; Williams, R. J. J. *Thermosetting Polymers*; Dekker: New York, 2002.
(31) Girard-Reydet, E.; Sévignon, A.; Pascault, J. P.; Hoppe, C. E.; Galante, M. J.; Oyanguren, P. A.; Williams, R. J. J. *Macromol. Chem. Phys.* **2002**, *203*, 947.
(32) Hoppe, C. E.; Galante, M. J.; Oyanguren, P. A.; Williams, R. J. J.; Girard-Reydet, E.; Pascault, J. P. *Polym. Eng. Sci.* **2002**, *42*, 2361.
(33) Rico, M.; López, J.; Montero, B.; Bellas, R. *Eur. Polym. J.* **2012**, *48*, 1660.
(34) Galante, M. J.; Oyanguren, P. A.; Andromaque, K.; Frontini, P. M.; Williams, R. J. J. *Polym. Int.* **1999**, *48*, 642.
(35) González García, F.; Soares, B. G.; Williams, R. J. J. *Polym. Int.* **2002**, *51*, 1340.
(36) Hashimoto, T.; Fujimura, M.; Kawai, H. *Macromolecules* **1980**, *13*, 1660.
(37) Dean, J. M.; Lipic, P. M.; Grubbs, R. B.; Cook, R. F.; Bates, F. S. *J. Polym. Sci., Part B: Polym. Phys.* **2001**, *39*, 2996.
(38) Lonetti, B.; Tsigkri, A.; Lang, P. R.; Stellbrink, J.; Willner, L.; Kohlbrecher, J.; Lettinga, M. P. *Macromolecules* **2011**, *44*, 3583.
(39) Bhargava, P.; Zheng, J. X.; Li, P.; Quirk, R. P.; Harris, F. W.; Cheng, S. Z. D. *Macromolecules* **2006**, *39*, 4880.
(40) Sota, N.; Saijo, K.; Hasegawa, H.; Hashimoto, T.; Amemiya, Y.; Ito, K. *Macromolecules* **2013**, *46*, 2298−2316.
(41) Kinning, D. J.; Thomas, E. L. *Macromolecules* **1984**, *17*, 1712.
(42) Ritzenthaler, S.; Girard-Reydet, E.; Pascault, J. P. *Polymer* **2000**, *41*, 6375.